

KAE: KOLMOGOROV-ARNOLD AUTO-ENCODER FOR REPRESENTATION LEARNING

Fangchen Yu¹, Ruilizhen Hu¹, Yidong Lin¹, Yuqi Ma¹, Zhenghao Huang¹, Wenyu Li^{1,2*}

¹ The Chinese University of Hong Kong, Shenzhen

² Shenzhen Research Institute of Big Data

ABSTRACT

The Kolmogorov-Arnold Network (KAN) has recently gained attention as an alternative to traditional multi-layer perceptrons (MLPs), offering improved accuracy and interpretability by employing learnable activation functions on edges. In this paper, we introduce the Kolmogorov-Arnold Auto-Encoder (KAE), which integrates KAN with autoencoders (AEs) to enhance representation learning for retrieval, classification, and denoising tasks. Leveraging the flexible polynomial functions in KAN layers, KAE captures complex data patterns and non-linear relationships. Experiments on benchmark datasets demonstrate that KAE improves latent representation quality, reduces reconstruction errors, and achieves superior performance in downstream tasks such as retrieval, classification, and denoising, compared to standard autoencoders and other KAN variants. These results suggest KAE’s potential as a useful tool for representation learning. Our code is available at <https://github.com/SciYu/KAE/>.

1 INTRODUCTION

Autoencoders (Hinton & Salakhutdinov, 2006; Berahmand et al., 2024) are a fundamental component of modern deep learning, serving as powerful tools for unsupervised representation learning. By compressing input data into a lower-dimensional latent space and subsequently reconstructing it, autoencoders facilitate a wide range of applications, including dimensionality reduction (Wang et al., 2016; Lin et al., 2020), image classification (Zhou et al., 2019; 2023), and data denoising (Gondara, 2016; Cui & Zdeborová, 2024). Their ability to learn meaningful representations from unlabelled data has positioned them as essential in various AI domains, from computer vision (Mishra et al., 2018; Takeishi & Kalousis, 2021) to natural language processing (Shen et al., 2020; Kim et al., 2021), significantly enhancing the performance of downstream tasks.

Traditional autoencoders typically leverage multi-layer perceptrons (MLPs), characterized by fully connected layers. In a conventional autoencoder, each layer computes its output as $y = \sigma(Wx + b)$, where σ denotes a fixed activation function, W is the learnable weight matrix, x represents the input, and b is the bias vector. The optimization of W is traditionally performed through black-box AI systems, limiting the adaptability of the activation function to the data’s underlying structure.

Recent advancements in alternative architectures, such as Kolmogorov-Arnold Networks (KANs) (Liu et al., 2024b;a), offer a compelling pathway for enhancing autoencoder performance. Unlike MLPs, KANs redefine the output as $y = f(x)$, where f is a learnable activation function. This shift enables the network to adaptively learn more complex representations, moving beyond the limitations of fixed functions and linear weights used in MLPs.

In this paper, we propose the Kolmogorov-Arnold Auto-Encoder (KAE), which integrates the strengths of KANs into the autoencoder framework to create a more robust model for representation learning. However, merely substituting MLP layers with KAN layers utilizing B-spline functions may result in only marginal gains or even a decline in performance. The efficacy of KANs heavily depends on the specific type of function employed within the KAN layer. To address this challenge, we introduce a well-defined KAE architecture that utilizes learnable polynomial functions, demonstrating promising improvements in representation learning.

*Corresponding author.

Our contributions are as follows:

- We introduce the Kolmogorov-Arnold Representation Theorem into the design of autoencoders, providing a theoretical basis for improving autoencoder performance.
- We investigate the role of activation functions in the KAN layers, identifying polynomial functions as a suitable choice for enhancing autoencoder performance.
- We demonstrate the superiority of the Kolmogorov-Arnold Auto-Encoder (KAE) through extensive experimental validation, showing improvements in both reconstruction quality and downstream application performance.

The remainder of the paper is organized as follows. Section 2 reviews related work. Section 3 details the proposed KAE model, and Section 4 provides a thorough empirical evaluation. Finally, Section 5 concludes the paper.

2 RELATED WORK

2.1 AUTOENCODERS (AES)

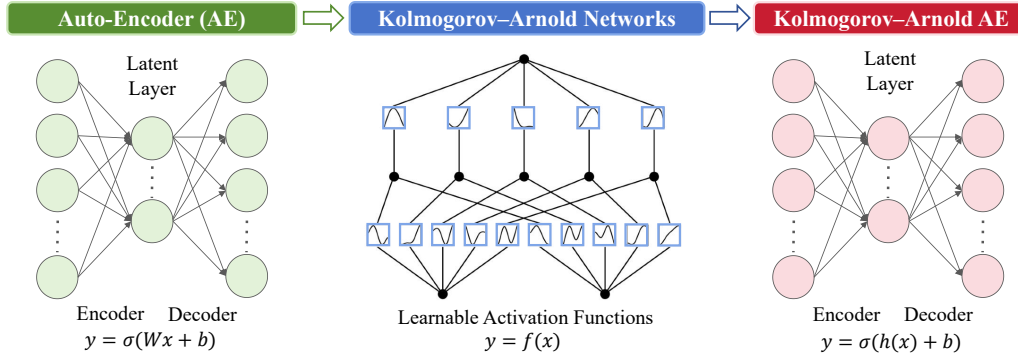


Figure 1: **Model Comparison of AE, KAN, and KAE.**

Autoencoders (Hinton & Salakhutdinov, 2006), as a framework of unsupervised learning, aim to learn a compressed representation of input data while minimizing reconstruction error. Traditionally, autoencoders rely on MLPs to achieve this task, where each layer applies a fixed non-linearity. However, this may limit the ability of the network to capture complex structures in the data.

Recent works have explored various autoencoder architectures, including Variational Auto-Encoders (VAEs) (Kingma, 2013; Kingma et al., 2019) and Denoising Auto-Encoders (DAEs) (Savinov et al., 2022; Wu et al., 2023), which introduce stochasticity and robustness to noise, respectively. Nevertheless, most of these architectures rely on fixed activation functions, which may limit their flexibility in representing complex functions.

As shown in Fig. 1, an autoencoder consists of two main parts:

- **Encoder:** This part compresses the input into a latent-space representation.
- **Decoder:** This part reconstructs the input data from the latent-space representation.

A common application of autoencoders is representation learning, where latent representations are learned and can be used for tasks such as image classification (Zhou et al., 2023), text classification (Xu & Tan, 2019), cross-modal learning (Dong et al., 2023), and other applications, particularly beneficial for high-dimensional data analysis. Another key feature of autoencoders is their ability to reduce noise in data (Bajaj et al., 2020). By inputting noisy data, the pre-trained autoencoder can remove the noise, producing clean outputs, which makes it a powerful tool for data denoising.

2.2 KOLMOGOROV-ARNOLD NETWORKS (KANs)

Kolmogorov-Arnold Networks (KANs) (Liu et al., 2024b;a) provide a flexible way to model non-linear relationships by using learnable activation functions rather than fixed ones. Inspired by the Kolmogorov-Arnold representation theorem (Kolmogorov, 1961; Braun & Griebel, 2009), KANs approximate any continuous multivariate function using a sum of univariate functions, providing a theoretically grounded approach to function approximation. In practice, KANs allow each layer to learn its own activation function, making them adaptable to non-linear data. KANs have been shown to outperform MLPs in various applications (Xu et al., 2024; Bozorgasl & Chen, 2024).

2.2.1 KOLMOGOROV-ARNOLD REPRESENTATION THEOREM

The Kolmogorov-Arnold representation theorem (Kolmogorov, 1961; Braun & Griebel, 2009) is a fundamental result in mathematics, particularly in functional analysis and multivariate approximation theory. It provides key insights into representing multivariate continuous functions. Theorem 1 asserts that any continuous function of d variables can be represented as a finite sum of continuous univariate functions along with an additional continuous function.

Theorem 1 (Kolmogorov-Arnold Representation Theorem). *For any smooth function $f : [0, 1]^d \rightarrow \mathbb{R}$, there exist continuous functions $\phi_{k,j} : [0, 1] \rightarrow \mathbb{R}$ and $\Phi_k : \mathbb{R} \rightarrow \mathbb{R}$ such that:*

$$f(x_1, x_2, \dots, x_d) = \sum_{k=1}^{2d+1} \Phi_k \left(\sum_{j=1}^d \phi_{k,j}(x_j) \right). \quad (1)$$

This remarkable theorem involves the use of two primary types of functions: **inner functions** $\{\phi_{k,j}\}$ and **outer functions** $\{\Phi_k\}$, which motivates the design of the KAN network.

2.2.2 KAN NETWORK AND ITS APPLICATIONS

Inspired by Theorem 1, Liu et al. (2024b;a) proposed a novel KAN layer with d_{in} -dimensional inputs and d_{out} -dimensional outputs, defined as a matrix of 1D functions:

$$\Phi := \{\phi_{k,j}\}, \quad j = 1, 2, \dots, d_{\text{in}}, \quad k = 1, 2, \dots, d_{\text{out}},$$

where each function $\phi_{k,j}$ is a learnable univariate function. A general KAN network is formed by stacking L KAN layers. Given an input vector $x \in \mathbb{R}^d$, the output of KAN is

$$\text{KAN}(x) := (\Phi_{L-1} \circ \Phi_{L-2} \circ \dots \circ \Phi_1 \circ \Phi_0) \circ x, \quad (2)$$

where the Kolmogorov-Arnold representation in Eq. (1) can be viewed as a composition of two KAN layers: Φ_0 contains $(2d + 1) \cdot d$ functions, and Φ_1 contains $1 \cdot (2d + 1)$ functions.

Recently, KAN networks have been applied to various domains, including scientific discovery (Liu et al., 2024b;a), image segmentation (Li et al., 2024), image classification (Cheon, 2024), text classification (Imran & Ishmam, 2024), collaborative filtering (Xu et al., 2024), and others. KAN-based architectures, such as the Kolmogorov-Arnold Transformer (Yang & Wang, 2024) and U-KAN (Li et al., 2024), have also gained significant attention.

3 KOLMOGOROV-ARNOLD AUTO-ENCODER

3.1 KANs IN AUTOENCODERS

KANs have demonstrated potential for enhancing neural network architectures, but their application to autoencoders poses challenges. Specifically, the complexity introduced by learnable activation functions can result in overfitting or suboptimal performance if not carefully managed. To address this, we propose a novel autoencoder architecture that integrates KANs with polynomial-based activation functions, which we found to be more stable and effective for this task.

A concurrent work (Moradi et al., 2024) also introduces a KAN-based autoencoder. However, their approach employs B-spline functions in the KAN layer and adopts a KAN-ReLU-Dense structure in the encoder. In contrast, our architecture uses polynomial functions in the KAN layer, significantly reducing the number of hyperparameters and eliminating the need for dense layers. This design offers a more efficient and streamlined alternative.

3.2 OVERALL ARCHITECTURE

The key idea behind the Kolmogorov-Arnold Auto-Encoder (KAE) is to replace the MLP layers (fixed activation functions) in traditional autoencoders with KAN layers (learnable functions), as inspired by the Kolmogorov-Arnold representation theorem.

In a traditional autoencoder, the MLP consists of fully connected layers that apply a fixed activation function, such as ReLU or sigmoid, after a linear transformation. Given an input vector $x \in \mathbb{R}^d$, the encoder compresses the data into a lower-dimensional latent representation $z \in \mathbb{R}^k$, and the decoder reconstructs z back into the original space. This transformation is typically expressed as:

$$z = \sigma(Wx + b),$$

where W is the weight matrix, b is the bias, and σ is a fixed activation function.

In KAE, we replace the MLP layers with KAN layers, which use learnable activation functions as defined by the Kolmogorov-Arnold representation theorem. Instead of a fixed σ , each KAN layer dynamically learns its own activation function, enabling the model to capture complex, non-linear patterns. The encoder applies a series of KAN layers to map the input to the latent space:

$$z = f(x) := (\Phi_{L-1} \circ \Phi_{L-2} \circ \dots \circ \Phi_1 \circ \Phi_0) \circ x,$$

where each Φ_i represents a KAN layer composed of learnable univariate functions.

Similarly, the decoder ($y = g(z)$) uses KAN layers in reverse to reconstruct the data, providing greater flexibility and accuracy compared to standard MLP-based decoders. This architecture enables KAE to capture complex, non-linear relationships, enhancing the quality of the learned representations. As with standard autoencoders, we use the mean squared error (MSE) between the original and reconstructed data as the training loss.

3.3 POLYNOMIAL ACTIVATION FUNCTION

The autoencoder’s primary task is to ensure that the encoding and decoding functions are inverses of each other, i.e., $x \approx g(f(x))$ for all $x \in \mathbb{R}^d$. In a traditional autoencoder, the layers are fully connected, and this inversion property is straightforward to achieve. However, when using KAN layers, the choice of functions f and g becomes more nuanced. Naïvely replacing the MLP layer with a KAN layer does not produce satisfactory results, as shown in our evaluation in Section 4.

To ensure consistency between the encoder and decoder, we carefully design the $f(x)$ and $g(z)$ to be invertible, using polynomial approximations that are both smooth and differentiable. For a KAE layer with d_{in} -dimensional inputs and d_{out} -dimensional outputs, the output of $x \in \mathbb{R}^{d_{\text{in}}}$ is defined as:

$$\text{KAE}(x) := \sigma(h(x) + b) = \sigma((c_0 \mathbf{1}_{d_{\text{in}}} + c_1 x + c_2 x^2 + \dots + c_p x^p) + b), \quad (3)$$

where $\mathbf{1}_{d_{\text{in}}}$ is an all-ones vector and p is the order of the polynomials, treated as a hyperparameter in KAE. To maintain consistency with the MLP-based AE, we use the structure $\sigma(\cdot + b)$, replacing the Wx term with $h(x)$, resulting in $\sigma(h(x) + b)$ with the following advantages.

- Compared to the linear transformation Wx in MLPs, polynomial functions $h(x)$ introduce higher-order non-linear terms such as x^p , enabling the model to capture more complex, non-linear relationships in the data.
- The polynomial function includes a constant matrix $c_0 \in \mathbb{R}^{d_{\text{out}} \times d_{\text{in}}}$, providing more flexibility than the traditional bias term $b \in \mathbb{R}^{d_{\text{out}}}$, allowing the model to better adapt to shifts and variations in the data.

Notably, in the standard KAN (Liu et al., 2024b), the learnable function $h(x)$ is set as a B-spline function, while in FourierKAN (Xu et al., 2024) it is set as a Fourier function, and in WavKAN (Bozorgasl & Chen, 2024) it is set as a Wavelet function. Comparatively, our empirical validation shows that quadratic and cubic polynomial functions (with $p = 2, 3$) offer a more effective balance between flexibility and stability, improving the model’s ability to reconstruct data while maintaining the inversion property between the encoder and decoder.

4 EVALUATION

4.1 EXPERIMENTAL SETUP

To assess the effectiveness of the proposed Kolmogorov-Arnold Auto-Encoder (**KAE**), we conducted a series of experiments to address the following key objectives:

- **Reconstruction in representation learning:** Evaluating the model’s ability to effectively compress and decompress data by comparing reconstructed outputs to the original inputs.
- **Quality of latent representations:** Assessing the utility of learned representations in downstream tasks such as similarity search, image classification, and image denoising.
- **Model capacity:** Analyzing the model’s performance relative to the number of learnable parameters, providing insight into its capacity and efficiency.

We compared the proposed KAE¹ against the following baseline models:

- **Standard Auto-Encoder (AE)** (Hinton & Salakhutdinov, 2006): Utilizes the Sigmoid activation function.
- **Kolmogorov-Arnold Network (KAN)** (Liu et al., 2024b;a): Employs B-spline activation functions. The default parameters are consistent with the Efficient-KAN implementation², such as `grid_size = 5`, `spline_order = 3`, and `grid_range = [-1, 1]`.
- **FourierKAN** (Xu et al., 2024): Uses the default setting of the basic implementation of FourierKAN³ with `grid_size = 5`, adds bias, and does not apply smooth initialization.
- **WavKAN** (Bozorgasl & Chen, 2024): Implements the default configuration as the official code⁴, including Mexican hat wavelets as activation functions.

We employed several well-known image datasets for our evaluations, as summarized in Table 1.

Table 1: Statistics of the Image Datasets Used in Our Work.

Dataset	Image Type	Image Size	#Classes	#Training	#Test
MNIST (LeCun et al., 1998)	Grayscale handwritten digits	28×28	10	60,000	10,000
FashionMNIST (Xiao et al., 2017)	Grayscale images of clothing	28×28	10	60,000	10,000
CIFAR10 (Krizhevsky & Hinton, 2009)	RGB natural images	32×32	10	50,000	10,000
CIFAR100 (Krizhevsky & Hinton, 2009)	RGB natural images	32×32	100	50,000	10,000

Each experiment was repeated ten times with random seeds from 2,024 to 2,033, and the average results with standard deviation were reported. Models were trained using the Adam optimizer (Kingma, 2014), exploring four configurations of learning rate (1e-4 or 1e-5) and weight decay (1e-4 or 1e-5), with a batch size of 256 for 10 epochs. The best-performing configuration was reported.

All experiments were conducted using Python (version 3.10) and PyTorch 2.4 as the deep learning framework. Computations were performed on a ThinkStation equipped with an Intel i7-12700 CPU (2.1 GHz), 32GB of RAM, and an NVIDIA TITAN V GPU with 12GB of GPU memory.

4.2 RECONSTRUCTION QUALITY

Autoencoders perform the representation learning by compressing input data into a latent space (encoding) and then reconstructing it back (decoding). To assess how well different models perform this task, we compared their reconstruction error using the mean squared error (MSE) between the original input and the reconstructed output on the test set.

¹The implementation of KAE is provided at <https://github.com/SciYu/KAE>, which is built upon the TaylorKAN codebase (<https://github.com/Muyuzhierchengse/TaylorKAN>). In our experiments, the polynomial order p of the KAE is set to 1, 2, and 3, with the Sigmoid function used as σ .

²<https://github.com/Blealtan/efficient-kan>

³<https://github.com/GistNoesis/FourierKAN>

⁴<https://github.com/zavareh1/Wav-KAN>

For all models, we employed a shallow architecture consisting of three layers: $d_{\text{input}}-d_{\text{latent}}-d_{\text{output}}$, where d_{latent} represents the dimension of the compressed latent space. After training each model, a previously unseen test input x was passed through the network to obtain the latent representation y and the reconstructed output z . The reconstruction error was then calculated as the MSE, defined by $\|x - z\|^2$, and averaged across all test data batches.

Table 2 demonstrates the superiority of KAE compared to AE and KAN variants in terms of reconstruction error. The results highlight several key observations:

- **KAE vs AE:** Both KAN and KAE consistently deliver significantly lower reconstruction errors than AE in all settings, with the error reduction of KAE highlighted in the last row of Table 2.
- **KAE vs KAN:** The performance of KAN variants is highly dependent on the choice of activation function. The polynomial function used in our KAE model outperforms the B-spline function in KAN, the Fourier function in FourierKAN, and the wavelet function in WavKAN for this reconstruction task. Additionally, higher-order polynomial functions (i.e., $p = 3$) in KAE lead to better reconstruction performance.

Table 2: **Reconstruction Error Comparison Across Datasets for Different Latent Dimensions.** The best results are in **bold** and the second best are underlined. The last row shows the improvement of KAE models over standard autoencoders (AE).

Dataset	MNIST		FashionMNIST		CIFAR10		CIFAR100	
	16	32	16	32	16	32	16	32
AE	0.056 \pm 0.002	0.043 \pm 0.001	0.045 \pm 0.002	0.034 \pm 0.001	0.034 \pm 0.001	0.029 \pm 0.001	0.037 \pm 0.001	0.030 \pm 0.001
KAN	0.047 \pm 0.002	0.036 \pm 0.001	0.032 \pm 0.003	0.024 \pm 0.000	0.025 \pm 0.001	0.019 \pm 0.000	0.025 \pm 0.001	0.018 \pm 0.001
FourierKAN	0.042 \pm 0.003	0.031 \pm 0.003	0.031 \pm 0.001	0.024 \pm 0.001	0.031 \pm 0.002	0.023 \pm 0.001	0.029 \pm 0.001	0.022 \pm 0.001
WavKAN	0.175 \pm 0.002	0.161 \pm 0.002	0.099 \pm 0.001	0.089 \pm 0.000	0.035 \pm 0.001	0.025 \pm 0.000	0.036 \pm 0.001	0.026 \pm 0.000
KAE (p=1)	0.050 \pm 0.004	0.041 \pm 0.000	0.029 \pm 0.001	0.025 \pm 0.001	0.021 \pm 0.000	0.020 \pm 0.000	0.021 \pm 0.001	0.019 \pm 0.000
KAE (p=2)	0.026 \pm 0.002	0.017 \pm 0.001	0.020 \pm 0.000	0.016 \pm 0.001	0.017 \pm 0.001	0.013 \pm 0.000	0.017 \pm 0.001	0.013 \pm 0.000
KAE (p=3)	0.024 \pm 0.001	0.015 \pm 0.001	0.018 \pm 0.001	0.015 \pm 0.000	0.016 \pm 0.001	0.012 \pm 0.000	0.016 \pm 0.001	0.012 \pm 0.000
Improve	0.032 \downarrow	0.028 \downarrow	0.027 \downarrow	0.019 \downarrow	0.018 \downarrow	0.017 \downarrow	0.021 \downarrow	0.018 \downarrow

4.3 APPLICATIONS

To evaluate the quality of the compressed data, we applied the latent representations to several downstream tasks, including similarity search, image classification, and image denoising, demonstrating the high-quality representations learned by the proposed KAE models.

4.3.1 SIMILARITY SEARCH

A well-designed autoencoder, as a tool for dimensionality reduction, should preserve the distance relationships between samples from the input space to the latent space, making similarity search a suitable application for assessing this property.

For each experiment, we randomly selected a subset of 1,000 test samples as the test set. For each query, we computed the k nearest neighbors in the input space as the ground truth and compared it to the N nearest neighbors retrieved in the latent space. We calculated the recall, defined as the ratio of true top- k results within the top- N retrieved candidates, and reported it as Recall $k@N$. In our experiments, we set $k = 10$ and tested Recall $10@N$ (referred to as **Recall@N**) for all models. Each experiment was repeated 10 times with different random seeds, and we reported the averaged Recall with standard deviations.

Table 3 presents the Recall@10 results for various models across latent dimensions (16 and 32). Increasing the latent dimension from 16 to 32 significantly improved retrieval recall for all models, enhancing their distance-preserving properties and expressive power. Notably, the proposed KAE model consistently outperformed both the standard AE and KAN variants across all datasets and dimensions. Specifically, KAE ($p = 2$) achieved improvements of 0.242 and 0.206 in Recall@10 over AE for MNIST with latent dimensions of 16 and 32, respectively, with similar gains observed for FashionMNIST, CIFAR10, and CIFAR100 datasets.

Table 3: **Retrieval Recall@10 Comparison Across Datasets for Different Latent Dimensions.** The best results are in **bold** and the second best are underlined. The last row shows the improvement of KAE models over standard autoencoders (AE).

Dataset	MNIST		FashionMNIST		CIFAR10		CIFAR100	
	16	32	16	32	16	32	16	32
AE	0.354 \pm 0.017	0.483 \pm 0.008	0.401 \pm 0.016	0.526 \pm 0.009	0.368 \pm 0.026	0.472 \pm 0.012	0.380 \pm 0.015	0.477 \pm 0.009
KAN	0.457 \pm 0.015	0.552 \pm 0.016	0.495 \pm 0.023	0.578 \pm 0.004	0.377 \pm 0.015	0.496 \pm 0.007	0.391 \pm 0.009	0.512 \pm 0.007
FourierKAN	0.498 \pm 0.053	0.638 \pm 0.034	0.518 \pm 0.022	<u>0.615</u> \pm 0.018	0.258 \pm 0.041	0.406 \pm 0.028	0.316 \pm 0.026	0.435 \pm 0.019
WavKAN	0.259 \pm 0.037	0.447 \pm 0.018	0.387 \pm 0.015	0.488 \pm 0.006	0.258 \pm 0.016	0.428 \pm 0.012	0.259 \pm 0.013	0.430 \pm 0.011
KAE (p=1)	0.404 \pm 0.028	0.488 \pm 0.007	0.544 \pm 0.008	0.581 \pm 0.010	0.440 \pm 0.011	0.489 \pm 0.008	0.453 \pm 0.008	0.504 \pm 0.005
KAE (p=2)	0.596 \pm 0.019	0.689 \pm 0.011	0.607 \pm 0.010	0.661 \pm 0.007	0.525 \pm 0.021	0.631 \pm 0.011	0.544 \pm 0.013	0.639 \pm 0.007
KAE (p=3)	<u>0.554</u> \pm 0.013	<u>0.659</u> \pm 0.013	<u>0.521</u> \pm 0.006	0.582 \pm 0.006	<u>0.488</u> \pm 0.012	<u>0.597</u> \pm 0.010	<u>0.493</u> \pm 0.013	<u>0.586</u> \pm 0.012
Improve	0.242 \uparrow	0.206 \uparrow	0.206 \uparrow	0.135 \uparrow	0.157 \uparrow	0.159 \uparrow	0.164 \uparrow	0.162 \uparrow

As shown in Fig. 2, increasing the number of retrieved samples revealed that non-linear polynomial functions (e.g., KAE ($p = 2, 3$)) achieved competitive results. Especially on more complex datasets like CIFAR10 and CIFAR100, KAEs significantly outperformed FourierKAN and WavKAN, which exhibited lower recall values. This highlights the ability of KAEs to preserve the intrinsic structure of the data in the latent space, making them highly effective for similarity-based retrieval tasks.

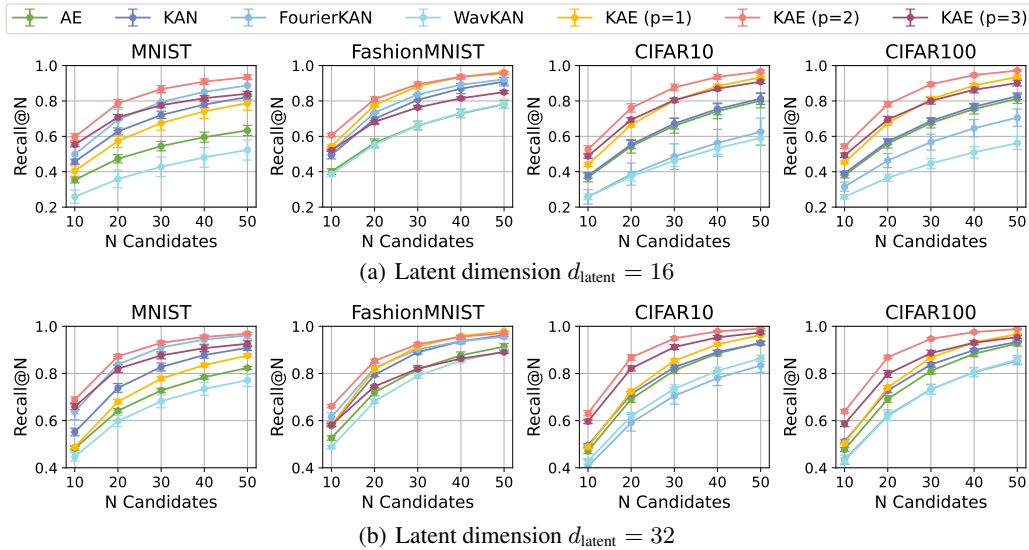


Figure 2: **Recall@N of Similarity Search Across Datasets for Different Latent Dimensions.**

4.3.2 IMAGE CLASSIFICATION

We further applied the learned latent representations to image classification using a nearest neighbor classifier. For each of the 10,000 test samples, the predicted label was assigned based on the nearest sample in the latent space with the smallest Euclidean distance. We then compared the predicted labels with the ground truth, averaging the classification accuracy across all test samples.

Table 4 shows that KAE models, particularly with the non-linear polynomial function ($p = 3$), achieved the highest classification accuracy across all datasets. This contrasts with similarity search, where $p = 2$ performed best. The difference in performance may due to the nature of each task:

- In similarity search, KAE ($p = 2$) better preserves the distance relationships between neighbors, which is crucial for retrieving similar samples.
- In image classification, KAE ($p = 3$) captures more complex, non-linear relationships, enabling better discrimination between class boundaries and improving classification accuracy.

Table 4: **Classification Accuracy Comparison Across Datasets for Different Latent Dimensions.** The best results are in **bold** and the second best are underlined. The last row shows the improvement of KAE models over standard autoencoders (AE).

Dataset	MNIST		FashionMNIST		CIFAR10		CIFAR100	
	16	32	16	32	16	32	16	32
AE	0.853 \pm 0.014	0.916 \pm 0.007	0.737 \pm 0.007	0.781 \pm 0.004	0.243 \pm 0.010	0.283 \pm 0.006	0.076 \pm 0.005	0.101 \pm 0.003
KAN	0.883 \pm 0.012	0.931 \pm 0.006	0.752 \pm 0.007	0.786 \pm 0.002	0.244 \pm 0.006	0.290 \pm 0.004	0.080 \pm 0.003	0.110 \pm 0.003
FourierKAN	0.859 \pm 0.047	0.947 \pm 0.012	0.735 \pm 0.008	0.795 \pm 0.007	0.164 \pm 0.016	0.246 \pm 0.017	0.040 \pm 0.007	0.085 \pm 0.009
WavKAN	0.649 \pm 0.056	0.887 \pm 0.012	0.679 \pm 0.009	0.751 \pm 0.004	0.189 \pm 0.008	0.272 \pm 0.005	0.043 \pm 0.003	0.096 \pm 0.003
KAE (p=1)	0.802 \pm 0.013	0.868 \pm 0.008	0.751 \pm 0.005	0.773 \pm 0.005	0.262 \pm 0.006	0.282 \pm 0.003	0.087 \pm 0.003	0.104 \pm 0.002
KAE (p=2)	<u>0.929</u> \pm 0.011	<u>0.963</u> \pm 0.002	<u>0.801</u> \pm 0.003	<u>0.824</u> \pm 0.003	<u>0.304</u> \pm 0.010	<u>0.338</u> \pm 0.004	<u>0.124</u> \pm 0.006	<u>0.148</u> \pm 0.002
KAE (p=3)	0.940 \pm 0.005	0.964 \pm 0.002	0.805 \pm 0.004	0.826 \pm 0.002	0.315 \pm 0.009	0.354 \pm 0.004	0.131 \pm 0.005	0.154 \pm 0.003
Improve	0.087 \uparrow	0.048 \uparrow	0.068 \uparrow	0.045 \uparrow	0.072 \uparrow	0.071 \uparrow	0.055 \uparrow	0.053 \uparrow

4.3.3 IMAGE DENOISING

Image denoising is a natural extension of autoencoder applications, used to evaluate the robustness of learned models. By adding noise to the input images, we can assess the model’s ability to remove noise through compression and reconstruction, using the mean squared error (MSE) between the denoised and original clean images as denoising error. We applied two common types of noise:

- **Gaussian noise:** Added Gaussian noise $\mathcal{N}(0, 0.1^2)$ to the clean images.
- **Salt-and-Pepper noise:** Randomly set pixels to 0 or 1 with a probability of 0.05.

Results in Table 5 show that both $p = 2$ and $p = 3$ of KAE consistently achieved the lowest denoising errors across all datasets, mirroring their strong performance in reconstruction. This indicates that the KAE models not only excel in image reconstruction but are also highly effective in removing noise, demonstrating their robustness in preserving the underlying structure of data. The consistent performance across different types of noise further highlights the KAE models’ ability to generalize well to varying noise conditions, making them superior to both the standard AE and KAN models.

Table 5: **Denoising Error Comparison Across Datasets for Different Latent Dimensions.** The best results are in **bold** and the second best are underlined. The last row shows the improvement of KAE models over standard autoencoders (AE).

Dataset	MNIST		FashionMNIST		CIFAR10		CIFAR100	
	16	32	16	32	16	32	16	32
<i>I. Gaussian Noise</i>								
AE	0.065 \pm 0.002	0.053 \pm 0.001	0.056 \pm 0.002	0.044 \pm 0.001	0.044 \pm 0.001	0.038 \pm 0.001	0.047 \pm 0.001	0.040 \pm 0.001
KAN	0.058 \pm 0.002	0.046 \pm 0.001	0.043 \pm 0.003	0.034 \pm 0.000	0.035 \pm 0.001	0.029 \pm 0.000	0.034 \pm 0.001	0.028 \pm 0.001
FourierKAN	0.063 \pm 0.002	0.054 \pm 0.001	0.049 \pm 0.001	0.041 \pm 0.001	0.048 \pm 0.002	0.041 \pm 0.001	0.047 \pm 0.001	0.040 \pm 0.001
WavKAN	0.188 \pm 0.003	0.174 \pm 0.004	0.115 \pm 0.002	0.105 \pm 0.001	0.045 \pm 0.001	0.035 \pm 0.000	0.046 \pm 0.001	0.037 \pm 0.000
KAE (p=1)	0.058 \pm 0.004	0.051 \pm 0.000	0.038 \pm 0.001	0.035 \pm 0.001	0.031 \pm 0.000	0.030 \pm 0.000	0.031 \pm 0.001	0.029 \pm 0.000
KAE (p=2)	<u>0.038</u> \pm 0.002	<u>0.027</u> \pm 0.001	<u>0.030</u> \pm 0.000	<u>0.026</u> \pm 0.001	0.027 \pm 0.001	<u>0.023</u> \pm 0.000	0.026 \pm 0.001	0.022 \pm 0.000
KAE (p=3)	0.034 \pm 0.001	0.025 \pm 0.001	0.029 \pm 0.001	0.025 \pm 0.000	0.027 \pm 0.001	0.022 \pm 0.000	0.026 \pm 0.001	0.022 \pm 0.000
Improve	0.031 \downarrow	0.028 \downarrow	0.027 \downarrow	0.019 \downarrow	0.017 \downarrow	0.016 \downarrow	0.021 \downarrow	0.018 \downarrow
<i>II. Salt-and-Pepper Noise</i>								
AE	0.092 \pm 0.002	0.082 \pm 0.001	0.078 \pm 0.001	0.069 \pm 0.001	0.058 \pm 0.001	0.053 \pm 0.001	0.061 \pm 0.001	0.055 \pm 0.001
KAN	0.086 \pm 0.002	0.075 \pm 0.001	0.067 \pm 0.002	0.060 \pm 0.000	0.050 \pm 0.001	0.045 \pm 0.000	0.050 \pm 0.001	0.045 \pm 0.000
FourierKAN	0.087 \pm 0.001	0.080 \pm 0.002	0.071 \pm 0.001	0.065 \pm 0.001	0.065 \pm 0.001	0.059 \pm 0.001	0.064 \pm 0.001	0.059 \pm 0.001
WavKAN	0.207 \pm 0.006	0.199 \pm 0.013	0.139 \pm 0.005	0.127 \pm 0.003	0.059 \pm 0.001	0.051 \pm 0.000	0.061 \pm 0.001	0.052 \pm 0.000
KAE (p=1)	0.085 \pm 0.003	0.080 \pm 0.000	0.063 \pm 0.001	0.061 \pm 0.001	0.047 \pm 0.000	0.046 \pm 0.000	0.048 \pm 0.000	0.046 \pm 0.000
KAE (p=2)	<u>0.070</u> \pm 0.002	0.061 \pm 0.001	0.057 \pm 0.000	<u>0.054</u> \pm 0.000	0.044 \pm 0.001	0.040 \pm 0.000	0.044 \pm 0.000	0.040 \pm 0.000
KAE (p=3)	0.068 \pm 0.001	0.061 \pm 0.001	0.057 \pm 0.001	0.053 \pm 0.000	0.044 \pm 0.001	0.040 \pm 0.000	0.044 \pm 0.000	0.040 \pm 0.000
Improve	0.024 \downarrow	0.021 \downarrow	0.021 \downarrow	0.016 \downarrow	0.014 \downarrow	0.013 \downarrow	0.017 \downarrow	0.015 \downarrow

4.4 PERFORMANCE ANALYSIS

Convergence Analysis. We measured the test loss as the average MSE between the reconstructed and original data in the test set. Fig. 3 illustrates the faster convergence of our KAE models with $p = 2$ or 3 , which converge within approximately 10 epochs and achieve the lowest test loss. In contrast, other models, particularly WavKAN and AE, struggle to converge even after 50 epochs.

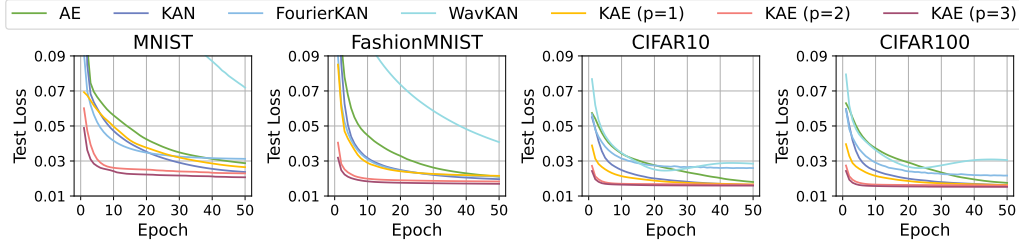


Figure 3: **Convergence Analysis of Test Loss Across Datasets for Latent Dimension $d_{\text{latent}} = 16$.**

Model Capacity Analysis. As shown in Fig. 4, our KAE models strike a balance between efficiency and accuracy, with the following key observations:

- **Training Efficiency:** While KAE models are not the fastest, they complete training in 30-36 seconds, only marginally slower than the fastest models, and significantly faster than two models with similar parameter counts, i.e., WavKAN and AE-S.
- **Classification Accuracy:** KAE models with $p = 2, 3$ use much fewer parameters (75-101K) while achieving higher accuracy compared to KAN (250K) and FourierKAN (251K).
- **Model Parameters:** When comparing models with similar parameter counts, KAE outperforms both WavKAN and AE-S in terms of training speed and performance. Even when the parameters of AE models are doubled, KAE still surpasses AE-B.

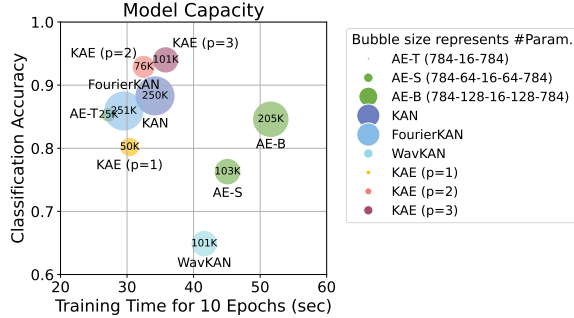


Figure 4: **Model Capacity Analysis on the MNIST Dataset with Latent Dimension $d_{\text{latent}} = 16$.** Bubble size represents the number of learnable parameters. For AE models, T = Tiny, S = Small, and B = Base.

5 CONCLUSION

In this paper, we introduced the Kolmogorov-Arnold Auto-Encoder (KAE), which integrates the Kolmogorov-Arnold Network (KAN) with autoencoders (AEs) to create a useful and flexible framework for representation learning. By incorporating KAN’s learnable polynomial activation functions into the AE structure, KAE effectively captures complex, non-linear relationships in the data, outperforming standard AEs. Our experiments on benchmark datasets highlight KAE’s superiority in reconstruction quality and downstream applications such as similarity search, image classification, and image denoising. Our analysis further demonstrates KAE’s greater capacity, especially through its learned polynomial activation functions.

Looking ahead, future work will focus on several key directions. First, we plan to combine the KAE architecture with autoencoder variants, such as Variational Auto-Encoders (VAE) (Kingma, 2013). Second, we aim to scale KAE to deeper architectures by incorporating KAN-based CNN layers and techniques like residual connections, enabling it to handle more complex datasets. Third, exploring alternative activation functions enhances the model’s flexibility. Finally, applying KAE to challenging real-world tasks, such as image generation, will offer deeper insights into its robustness and adaptability, further demonstrating its potential in practical applications.

REFERENCES

- Komal Bajaj, Dushyant Kumar Singh, and Mohd Aquib Ansari. Autoencoders based deep learner for image denoising. *Procedia Computer Science*, 171:1535–1541, 2020.
- Kamal Berahmand, Fatemeh Daneshfar, Elaheh Sadat Salehi, Yuefeng Li, and Yue Xu. Autoencoders and their applications in machine learning: a survey. *Artificial Intelligence Review*, 57(2): 28, 2024.
- Zavareh Bozorgasl and Hao Chen. Wav-kan: Wavelet kolmogorov-arnold networks. *arXiv preprint arXiv:2405.12832*, 2024.
- Jürgen Braun and Michael Griebel. On a constructive proof of kolmogorov’s superposition theorem. *Constructive Approximation*, 30:653–675, 2009.
- Minjong Cheon. Kolmogorov-arnold network for satellite image classification in remote sensing. *arXiv preprint arXiv:2406.00600*, 2024.
- Hugo Cui and Lenka Zdeborová. High-dimensional asymptotics of denoising autoencoders. *Advances in Neural Information Processing Systems*, 36, 2024.
- Runpei Dong, Zekun Qi, Linfeng Zhang, Junbo Zhang, Jianjian Sun, Zheng Ge, Li Yi, and Kaisheng Ma. Autoencoders as cross-modal teachers: Can pretrained 2d image transformers help 3d representation learning? In *11th International Conference on Learning Representations*, 2023.
- Lovedeep Gondara. Medical image denoising using convolutional denoising autoencoders. In *2016 IEEE 16th International Conference on Data Mining Workshops*, pp. 241–246. IEEE, 2016.
- Geoffrey E Hinton and Ruslan R Salakhutdinov. Reducing the dimensionality of data with neural networks. *Science*, 313(5786):504–507, 2006.
- Abdullah Al Imran and Md Farhan Ishmam. Leveraging fourierkan classification head for pre-trained transformer-based text classification. *arXiv preprint arXiv:2408.08803*, 2024.
- Jaehyeon Kim, Jungil Kong, and Juhee Son. Conditional variational autoencoder with adversarial learning for end-to-end text-to-speech. In *International Conference on Machine Learning*, pp. 5530–5540. PMLR, 2021.
- Diederik P Kingma. Auto-encoding variational bayes. *arXiv preprint arXiv:1312.6114*, 2013.
- Diederik P Kingma. Adam: A method for stochastic optimization. *arXiv preprint arXiv:1412.6980*, 2014.
- Diederik P Kingma, Max Welling, et al. An introduction to variational autoencoders. *Foundations and Trends® in Machine Learning*, 12(4):307–392, 2019.
- Andreï Nikolaevich Kolmogorov. *On the representation of continuous functions of several variables by superpositions of continuous functions of a smaller number of variables*. American Mathematical Society, 1961.
- Alex Krizhevsky and Geoffrey Hinton. Learning multiple layers of features from tiny images. 2009.
- Yann LeCun, Léon Bottou, Yoshua Bengio, and Patrick Haffner. Gradient-based learning applied to document recognition. *Proceedings of the IEEE*, 86(11):2278–2324, 1998.
- Chenxin Li, Xinyu Liu, Wuyang Li, Cheng Wang, Hengyu Liu, and Yixuan Yuan. U-kan makes strong backbone for medical image segmentation and generation. *arXiv preprint arXiv:2406.02918*, 2024.
- Eugene Lin, Sudipto Mukherjee, and Sreeram Kannan. A deep adversarial variational autoencoder model for dimensionality reduction in single-cell rna sequencing analysis. *BMC Bioinformatics*, 21:1–11, 2020.
- Ziming Liu, Pingchuan Ma, Yixuan Wang, Wojciech Matusik, and Max Tegmark. Kan 2.0: Kolmogorov-arnold networks meet science. *arXiv preprint arXiv:2408.10205*, 2024a.

- Ziming Liu, Yixuan Wang, Sachin Vaidya, Fabian Ruele, James Halverson, Marin Soljačić, Thomas Y Hou, and Max Tegmark. Kan: Kolmogorov-arnold networks. *arXiv preprint arXiv:2404.19756*, 2024b.
- Ashish Mishra, Shiva Krishna Reddy, Anurag Mittal, and Hema A Murthy. A generative model for zero shot learning using conditional variational autoencoders. In *Proceedings of the IEEE Conference on Computer Vision and Pattern Recognition Workshops*, pp. 2188–2196, 2018.
- Mohammadamin Moradi, Shirin Panahi, Erik Bollt, and Ying-Cheng Lai. Kolmogorov-arnold network autoencoders. *arXiv preprint arXiv:2410.02077*, 2024.
- Nikolay Savinov, Junyoung Chung, Mikolaj Binkowski, Erich Elsen, and Aaron van den Oord. Step-unrolled denoising autoencoders for text generation. In *10th International Conference on Learning Representations*, 2022.
- Tianxiao Shen, Jonas Mueller, Regina Barzilay, and Tommi Jaakkola. Educating text autoencoders: Latent representation guidance via denoising. In *International Conference on Machine Learning*, pp. 8719–8729. PMLR, 2020.
- Naoya Takeishi and Alexandros Kalousis. Physics-integrated variational autoencoders for robust and interpretable generative modeling. *Advances in Neural Information Processing Systems*, 34: 14809–14821, 2021.
- Yasi Wang, Hongxun Yao, and Sicheng Zhao. Auto-encoder based dimensionality reduction. *Neurocomputing*, 184:232–242, 2016.
- QuanLin Wu, Hang Ye, Yuntian Gu, Huishuai Zhang, Liwei Wang, and Di He. Denoising masked autoencoders help robust classification. In *11th International Conference on Learning Representations*, 2023.
- Han Xiao, Kashif Rasul, and Roland Vollgraf. Fashion-mnist: a novel image dataset for benchmarking machine learning algorithms. *arXiv preprint arXiv:1708.07747*, 2017.
- Jinfeng Xu, Zheyu Chen, Jinze Li, Shuo Yang, Wei Wang, Xiping Hu, and Edith C-H Ngai. Fourierkan-gcf: Fourier kolmogorov-arnold network—an effective and efficient feature transformation for graph collaborative filtering. *arXiv preprint arXiv:2406.01034*, 2024.
- Weidi Xu and Ying Tan. Semisupervised text classification by variational autoencoder. *IEEE Transactions on Neural Networks and Learning Systems*, 31(1):295–308, 2019.
- Xingyi Yang and Xinchao Wang. Kolmogorov-arnold transformer. *arXiv preprint arXiv:2409.10594*, 2024.
- Lei Zhou, Huidong Liu, Joseph Bae, Junjun He, Dimitris Samaras, and Prateek Prasanna. Self pre-training with masked autoencoders for medical image classification and segmentation. In *2023 IEEE 20th International Symposium on Biomedical Imaging*, pp. 1–6. IEEE, 2023.
- Peicheng Zhou, Junwei Han, Gong Cheng, and Baochang Zhang. Learning compact and discriminative stacked autoencoder for hyperspectral image classification. *IEEE Transactions on Geoscience and Remote Sensing*, 57(7):4823–4833, 2019.